

VARIATIONS AMONG DARK-TONED INTRACRATER DEPOSITS IN AMAZONIS PLANITIA. R.D. Schneider and V.E. Hamilton, Hawai'i Institute of Geophysics and Planetology, University of Hawai'i, 2525 Correa Road, Honolulu, HI, 96822 (romy@higp.hawaii.edu).

Introduction: Intracrater dark-toned deposits are common on the Martian surface, and are typified by distinctly lower albedos and higher thermal inertias relative to their surroundings [1,2]. Several regions on Mars have markedly higher concentrations of dark intracrater features, and studies of these areas can yield important information on regional wind regimes as well as sand supply and composition [3]. One particular study of some of these regions determined that the intracrater deposits are composed of sand-sized lithic particles that are locally derived [4]. One purpose of this study is to build on those results by investigating an additional region in detail. For this study, we examined 21 dark intracrater deposits in Amazonis Planitia (Figure 1). Here we present visible and spectral variations among the dark toned deposits, using data from the Mars Odyssey Thermal Emission Imaging System (THEMIS) and Mars Global Surveyor Thermal Emission Spectrometer (TES).

Data: The THEMIS infrared subsystem is a multispectral imager that provides mineralogic and atmospheric information at nine wavelengths between 6.78 – 15 μm , in ~ 32 km wide swaths at a spatial resolution of 100 m [5]. THEMIS also is equipped with a visible wavelength imaging system that acquires images with ~ 19 m spatial resolution at five wavelengths from 0.425 – 0.860 μm [5]. TES is a hyperspectral, interferometric spectrometer with selectable ~ 5 or ~ 10 cm^{-1} sampling between ~ 5 – 50 μm [6]. TES also contains broadband visible (0.3 – 2.7 μm) and thermal (5 – 100 μm) bolometers; these subsystems are used to examine albedo and thermophysical properties of the Martian surface [6].

Methods: We first examined all resolvable craters ($> \sim 5$ km) in the Amazonis Planitia region for low albedo anomalies using TES and Viking IRTM albedo as well as THEMIS visible images. We found 21 intracrater dark-toned deposits in all, in craters that ranged in size from ~ 10 -100 km. Of these, 7 dark-toned deposits were associated with dark-toned wind streaks that emanated from the crater, always with a NE-SW orientation. All of the wind streaks are thermally distinct in IR images; two of the wind streaks are discernible only in daytime IR images while the rest are visible in both day- and nighttime IR images (Figures 3 and 5). Two intracrater deposits display dune forms at THEMIS visible image resolution (Figure 2), and one of these also is associated with a wind streak.

Next, we examined THEMIS day- and nighttime IR images of each crater and its associated dark-toned deposit. Every intracrater deposit appeared as a distinct thermal anomaly (hotter than the rest of the crater floor) both during the day and at night. For each deposit, we chose the THEMIS daytime IR image with the maximum brightness temperature and the best coverage of the deposit to investigate the spectral properties of the area. For each of these images, we produced decorrelation stretch (DCS) images to highlight the spectral variations between the deposit and the rest of the crater and its surrounding terrain. Based on the spectral variations in these DCS images, we identified three types of deposits. The intracrater deposits of the first group show a strong spectral difference compared to the rest of the crater and surrounding terrain (Figure 3), most notably pink to yellow colors in the 975 DCS image (numbers represent the IR bands used for red, green, and blue, respectively, in the image) and pink to blue colors in the 864 DCS image. The second group of intracrater deposits show much less spectral difference compared with the surrounding terrain than group 1 in DCS images, as shown in Figure 4. The last group of deposits is typified by a yellowish color in a 642 DCS image, in contrast to the usual cyan color exhibited by the other two groups in a 642 DCS. In addition, in the 975 and 864 DCS images, the deposits in this group have low spectral difference with the surrounding terrain, similar to deposits in group 2. Figure 5 illustrates the spectral color difference in DCS image 642 for a typical group 3 deposit compared to a typical group 1 deposit. The distributions of the intracrater deposits from the three groups are shown in Figure 1.

Conclusions and Further Work: Our initial analysis with THEMIS data indicates that there are both visual and spectral variations among the 21 intracrater deposits found in Amazonis Planitia. Generally there appear to be three spectral types of intracrater deposits. Although these spectral differences may represent compositional differences among the deposits, other possibilities exist as well. The lower spectral contrast of the group 2 deposits could be due to a very thin layer of dust over the deposit, much like the optically thin layer of dust that was found to partly cover one of the other intracrater deposits in this region [7]. The spectral differences evident in group 3 deposits could be due to similar effects, as well as unusual acquisition conditions, such as a low

incidence angle (i.e. late in the day). To distinguish between these effects and compositional differences we will extract TES and THEMIS apparent emissivity spectra for all the deposits. An overlying layer of dust or patches of dust within the deposit should correspond to higher emissivities at longer wavelengths ($> \sim 8 \mu\text{m}$), and lower emissivities at shorter wavelengths ($< \sim 8 \mu\text{m}$). Alternatively, compositional differences between the deposits will be manifested as differences in spectral shape.

In the future we will expand our analysis of the intracrater deposits with TES albedo and thermal inertia data to further investigate the mineralogy and grain size of each deposit. The ultimate goal of our study is to determine if all or some of the dark-toned intracrater deposits in the Amazonis Planitia region have a similar origin and/or geologic history.

References: [1] Christensen, P.R., (1983) *Icarus*, 56, 496-518. [2] Fenton, L.K. et al. (2003) *JGR*, 108, 5129-5167. [3] Edgett K.S. et al. (1994) *JGR*, 99, 1997-2018. [4] Aben, L.K. (2003) M.S. Thesis, ASU, 117pp. [5] Christensen, P. R. et al. (2003) *Science*, 300, 2056-2061. [6] Christensen, P. R. et al. (2001) *JGR*, 106, 23,823-23,871. [7] Schneider, R.D. et al. (2004) *LPSC XXXV*, Abs. #1470.

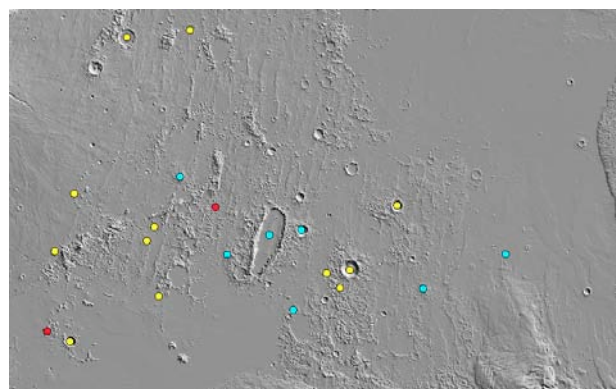


Figure 1. Distribution of intracrater dark-toned deposits in Amazonis Planitia. Upper left corner is $\sim 32^\circ \text{N}$, 156°E , lower right corner is $\sim 5^\circ \text{N}$, 209°E . Yellow corresponds to group 1, cyan to group 2, and red to group 3.

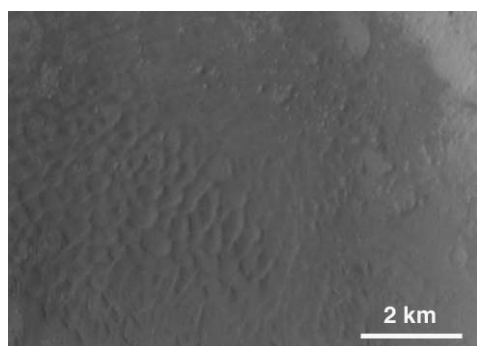


Figure 2. Dune forms in dark-toned deposit. Portion of THEMIS VIS image V10592013, band 3.

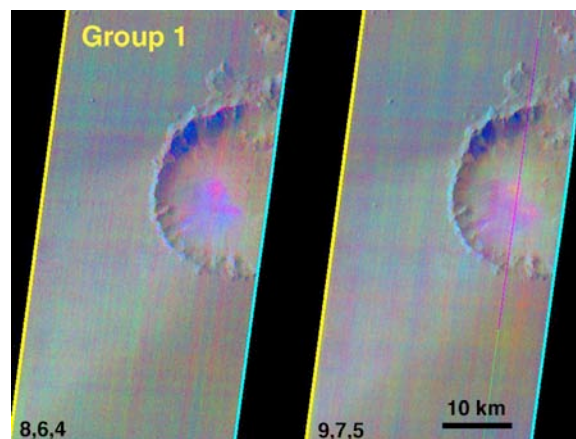


Figure 3. DCS images typical of group 1. Portion of THEMIS daytime IR image 102553005. Numbers in lower left corner of image indicate bands used for red, green, and blue, respectively.

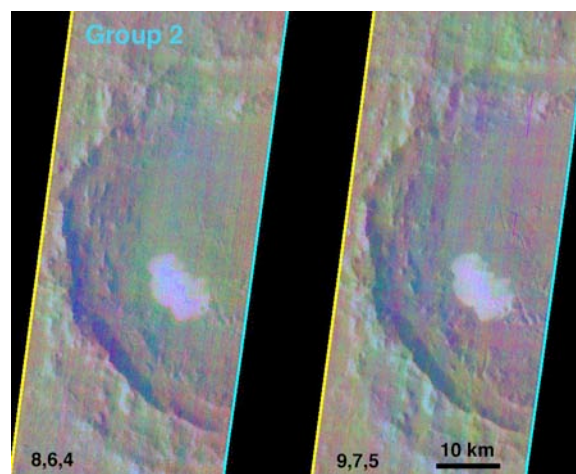


Figure 4. DCS images typical of group 2. Portion of THEMIS daytime IR image 109518012. Numbers in lower left corner of image indicate bands used for red, green, and blue, respectively.

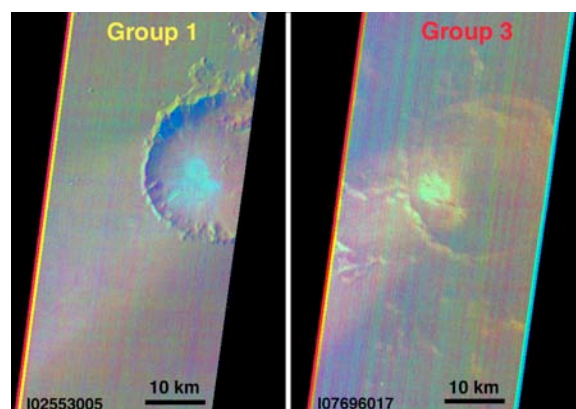


Figure 5. Comparison of DCS image 642 (red, green, blue) for groups 1 (left) and 3 (right). Both images are portions of the THEMIS daytime IR image number indicated in the lower left corner.